

---

# Semantically Controllable Scene Generation with Guidance of Explicit Knowledge

---

**Wenhao Ding**  
Carnegie Mellon University  
wenhaod@andrew.cmu.edu

**Bo Li**  
UIUC  
lbo@illinois.edu

**Kim Ji Eun**  
Robert Bosch LLC  
JiEun.Kim@us.bosch.com

**Ding Zhao**  
Carnegie Mellon University  
dingzhao@andrew.cmu.edu

## Abstract

Deep Generative Models (DGMs) are known for their superior capability in generating realistic data. Extending purely data-driven approaches, recent specialized DGMs may satisfy additional controllable requirements such as embedding a traffic sign in a driving scene, by manipulating patterns *implicitly* in the neuron or feature level. In this paper, we introduce a novel method to incorporate domain knowledge *explicitly* in the generation process to achieve semantically controllable scene generation. We categorize our knowledge into two types to be consistent with the composition of natural scenes, where the first type represents the property of objects and the second type represents the relationship among objects. We then propose a tree-structured generative model to learn complex scene representation, whose nodes and edges are naturally corresponding to the two types of knowledge respectively. Knowledge can be explicitly integrated to enable semantically controllable scene generation by imposing semantic rules on properties of nodes and edges in the tree structure. We construct a synthetic example to illustrate the controllability and explainability of our method in a clean setting. We further extend the synthetic example to realistic autonomous vehicle driving environments and conduct extensive experiments to show that our method efficiently identifies adversarial traffic scenes against different state-of-the-art 3D point cloud segmentation models satisfying the traffic rules specified as the explicit knowledge.

## 1 Introduction

The recent breakthrough in machine learning enables us to learn complex distributions behind data with sophisticated models. These models help us understand the data generation process, so as to realize controllable data generation Abdal et al. [2019], Tripp et al. [2020], Ding et al. [2021]. Deep Generative Models (DGMs) Goodfellow et al. [2014], Kingma and Welling [2013], Dinh et al. [2016], which approximate the data distribution with neural networks (NN), are representative methods to generate data targeting a specific style, category, or attribute. However, existing controllable generative models focus on manipulating implicit patterns in the neuron or feature level. For instance, Bau et al. [2020] dissects DGMs to build the relationship between neurons and generated data, while Plumerault et al. [2020] interpolates in the latent space to obtain vectors that control the poses of objects. One main limitation of these existing models is that they cannot explicitly incorporate unseen semantic rules, which may lead to meaningless generated data that violates common sense. For example, to build diverse scenes for training autonomous vehicles, the generated cars should follow semantic traffic rules and physical laws, which cannot be enforced by directly manipulating neurons.

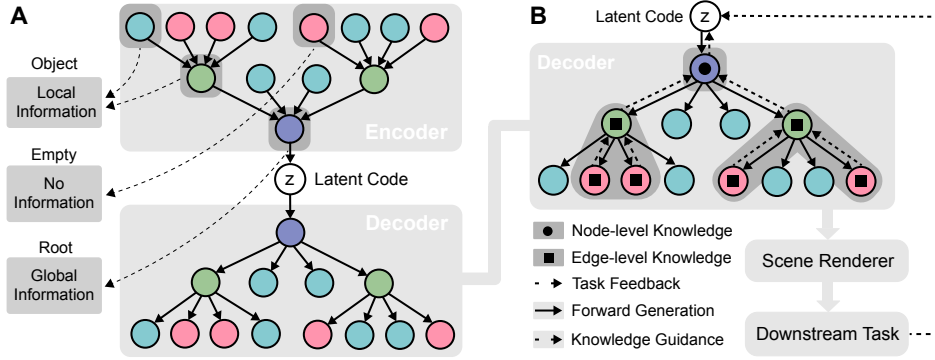


Figure 1: Diagram of proposed SCG. **A: Stage one.** Train T-VAE model to learn the representation of structured data. **B: Stage two.** Integrate node-level and edge-level knowledge during the generation and generate controllable samples for the downstream task.

In light of the limitations of previous work, we aim to develop a structured generative framework to integrate explicit knowledge Dienes and Perner [1999] during the generation process and thus control the generated scene to be compliant to semantic knowledge rules.

Natural scenes can be described with objects and their various relationship. Thus, in this paper, we categorize the semantic knowledge that describes scenes into two types, where the first type denoted as *node-level knowledge* represents the properties of single objects and the second type denoted as *edge-level knowledge* represents the relationship among objects. We also observe that tree structure is highly consistent with this categorization for constructing scenes, where nodes of the tree represent objects and edges the relationship. By automatically controlling the tree structure during the generation, we explicitly integrate the *node-level* and *edge-level* knowledge.

In detail, we propose a general framework, Semantically Controllable Generation (SCG), which consists of two stages as shown in Figure 1. In *stage one*, we train a tree-structured generative model that parameterizes nodes and edges of trees with NN to learn the representation of structured data. In *stage two*, explicit knowledge is applied to different levels of the tree to achieve semantically controllable scene generation for downstream tasks such as reducing the performance of recognition algorithms.

To verify the proposed SCG, we first construct a synthetic scene reconstruction example to illustrate the advantages of SCG and provide analysis on its controllability and explainability. With SCG, it is possible to generate natural scenes that follow semantic rules, e.g., boxes with the same color should be positioned together. To demonstrate the practicality of SCG, we conduct extensive experiments on adversarial LiDAR scene generation against state-of-the-art 3D segmentation models. We show that our generated traffic scenes successfully attack victim models and meanwhile follow the specified semantic rules. In addition, compared with traditional attack methods, scenes generated by our method achieve stronger adversarial transferability across different victim models. Our technical contributions are summarized below:

- (1) We propose a semantically controllable generative framework (SCG) via integrating explicit knowledge, and categorize the knowledge into two types according to the composition of scenes.
- (2) We propose a tree-structured generative model based on our knowledge categorization, and construct a synthetic example to demonstrate the effectiveness of our knowledge integration.
- (3) We propose the *first* semantic adversarial point cloud attack based on SCG, named *Scene Attack*, against state-of-the-art segmentation algorithms, demonstrating several important properties.

## 2 Preliminaries and Problem Formulation

### 2.1 Variational Auto-encoder (VAE)

VAE Kingma and Welling [2013] is a powerful DGM that combines auto-encoder and variational inference Blei et al. [2017]. It estimates a mapping between data  $x$  and latent code  $z$  to find the low-dimensional manifold of the data space, which makes it possible to convert structured data generation problems into continuous latent space searching. The objective function of training VAE

is to maximize a lower bound of the log-likelihood of training data, which is so-called Evidence Lower Bound (ELBO)

$$\text{ELBO} = -\mathbb{KL}(q(z|x; \phi) || p(z)) + \mathbb{E}_{q(z|x; \phi)} [\log p(x|z; \theta)] \quad (1)$$

where  $\mathbb{KL}$  is Kullback–Leibler (KL) divergence.  $q(z|x; \phi)$  is an encoder with parameters  $\phi$ , and  $p(x|z; \theta)$  is a decoder with parameters  $\theta$ . The prior distribution of the latent code  $p(z)$  is usually a Gaussian distribution for simplification of KL divergence calculation.

## 2.2 Proximal Algorithms

Proximal algorithms Parikh and Boyd [2014] are a type of optimization method that is constrained to a finite region at each step. In our setting, the explicit knowledge can be treated as the trusted region to limit and guide the optimization of the downstream task. The cost function  $f(x)$  of a optimization problem is separated into two parts  $f(x) = g(x) + h(x)$ , where  $h(x)$  is usually easy to optimize. The proximal mapping (or proximal operator) of the function  $h$  is

$$\text{prox}_h(x) = \arg \min_z \left( h(z) + \frac{1}{2} \|z - x\|_2^2 \right) \quad (2)$$

Then the proximal gradient algorithm has the following update:

$$x^{(t)} = \text{prox}_{\eta h}(x^{(t-1)} - \eta \nabla_x g(x^{(t-1)})) \quad (3)$$

where a gradient descend step is applied before the proximal operator. Then, the new candidate  $x^{(t)}$  will be obtained by solving the projection (2).

## 3 Semantically Controllable Generation for Scenes

We first describe the proposed tree-structured generative model used for learning the semantically controllable hierarchical representations. Then we explain the two types of knowledge to be integrated into tree structures and the generation algorithm that uses explicit knowledge as guidance.

### 3.1 Notations and Formulation

We define the tree of scene  $x \in \mathcal{X}$  in the data space and the latent code  $z \in \mathcal{Z}$  in the latent space. This paper aims to generate scene  $x$  that satisfies certain specified semantic rules  $Y_t$ , which are related to the downstream task  $t \in \mathcal{T}$ . We also assume the scene  $x$  is used to solve the downstream task  $t$  by minimizing an objective function  $L_t(x)$ .

### 3.2 Tree-structured Variational Auto-encoder (T-VAE)

One typical characteristic of natural scenes is the variable data dimension caused by the variable number of objects, which is impossible to represent with a fixed number of parameters as in traditional models Kingma and Welling [2013]. Besides, previous structured generative models Tan et al. [2021], Li et al. [2019] do not consider the hierarchy of natural scenes and incorporation of explicit knowledge. Based on the node-level and edge-level knowledge categorization, we propose a novel tree-structured model named T-VAE leveraging the stick-breaking construction Sethuraman [1994]. Suppose the scene has maximum width  $W$ , we have multiple divisions in 1D:

$$W = \sum_{i=1}^{K_n} w^{(n,i)}, \quad \forall n \in \{1, \dots, N\} \quad (4)$$

where  $(n, i)$  means the  $i$ -th node of the  $n$ -th level of the tree, and  $K_n$  is the total number of node in the  $n$ -th level. The index starts from 1 and the root node has index  $(1, 1)$ .  $w_{n,i}$  is a segment (also a node of the tree) obtained by continuously breaking the stick whose length is  $W$ . The recursive function of breaking the stick follows

$$w^{(n+1,j)} = w^{(n,i)} \alpha^{(n,i)}, \quad w^{(n+1,j+1)} = w^{(n,i)} (1 - \alpha^{(n,i)}) \quad (5)$$

where  $\alpha^{(n,i)} \in [0, 1]$  is the splitting ratio for  $w^{(n,i)}$  and  $j$  is the index in  $n + 1$ -th level. A 2-dimensional generation example is illustrated in Figure 2.



---

**Algorithm 1:** SCG Framework

---

<b>Input:</b> Dataset $\mathcal{D}$ , Task loss $\mathcal{L}_t(x)$ , Searching budget $B$ , Knowledge $Y_t$ <b>Output:</b> Generated scene $x_s$ <b>Stage 1:</b> Train T-VAE 1 Initialize model parameters $\{\theta, \phi\}$ 2 <b>for</b> $x$ in $\mathcal{D}$ <b>do</b> 3     Encode $z \leftarrow q(z x; \phi)$ 4     Decode $\hat{x} \leftarrow p(x z; \theta)$ 5     Update parameters $\{\theta, \phi\}$ by maximizing ELBO (9) 6 <b>end</b> 7 Store the mapping $p(x z; \theta)$	<b>Stage 2:</b> Knowledge-guided Generation 9 Initialize latent code $z_s \sim \mathcal{N}(0, \mathbf{I})$ 10 <b>while</b> $B$ is not used up <b>do</b> 11 <b>if</b> $\mathcal{L}_t(x)$ is differentiable <b>then</b> 12 $z_s \leftarrow z_s - \eta \nabla \mathcal{L}_t(p(x z_s; \theta))$ 13 <b>else</b> 14 $z_s \leftarrow$ Black-box optimization 15 <b>end</b> 16     Apply $Y_t$ to get $\mathcal{L}_Y(p(x z_s; \theta), Y_t(x))$ 17 $z_s \leftarrow \text{prox}_{\mathcal{L}_Y}(z_s)$ with GD 18 <b>end</b> 19 Decode the scene $x_s = p(x z_s; \theta)$
--	--

---

where  $N_m$  is the times that node  $m$  appears in the forward calculation and  $\mathbb{1}[\cdot]$  is the indicator function. In (11), we normalize the MSE with  $N_m$  instead of  $\sum_n^N K_n$  to avoid the influence caused by imbalanced node type in the tree.

The advantage of this hierarchical structure is that we only need to store the global information in the root node and use local information in other nodes, making the model easier to capture the feature from different scales in the scene. Moreover, this hierarchy makes it possible to explicitly apply semantic knowledge in *Stage 2*.

### 3.3 Knowledge-guided Generation

Suppose there is a function set  $\mathcal{F}$ , where the function  $f(A) \in \mathcal{F}$  returns true or false for a given input node  $A$  of a tree  $x$ . Then, we define the two types of propositional knowledge  $Y_t$  using the first-order logic Smullyan [1995] as following.

**Definition 1** The node-level knowledge  $y_n$  is denoted as  $f(A)$  for a function  $f \in \mathcal{F}$ , where  $A$  is a single node. The edge-level knowledge  $y_e$  is denoted as  $f_1(A) \rightarrow \forall i f_2(B_i)$  for two functions  $f_1, f_2 \in \mathcal{F}$ , where  $A$  is the parent node for  $B_i$ .

In the tree context,  $y_n$  describes the properties of a single node, and  $y_e$  describes the relationship between the parent node and its children. Finally, the knowledge set  $Y_t$  is constructed as  $Y_t = \{y_n^{(1)}, \dots, y_e^{(1)}, \dots\}$  and the operation  $Y_t(x)$  converts  $x$  to  $x'$ , which is a modified tree satisfying all propositions included in  $Y_t$ .

Then, we apply explicit knowledge to the decoder of T-VAE by extending the proximal gradient algorithm. Firstly, the original task objective  $\mathcal{L}_t(x)$  is augmented to

$$\mathcal{L}_a(x) = \mathcal{L}_t(x) + \mathcal{L}_Y(x, Y_t(x))$$

where  $\mathcal{L}_Y(x, Y_t(x))$  measures the distance between  $x$  and  $Y_t(x)$ . Specifically,  $y_n$  changes the property vector  $g$  of single node  $A$  in  $x$  to  $g'$  that make  $f(A)$  be true, and  $y_e$  traverses the tree  $x$  to find node  $A$  that satisfy  $f_1$  in  $y_e$  then change the type vector  $c$  or the property vector  $g$  of the children of  $A$  to  $c'$  and  $g'$  respectively. The reference vector  $c'$  and  $g'$  are related to the downstream task and are pre-defined in the function  $f$ . Then  $\mathcal{L}_Y$  consists of two parts, MSE is used between the property vector  $g$  and  $g'$ , and CE is used between the type vector  $c$  and  $c'$ .

For instance, the explicit knowledge described as “if one box is blue, its children nodes should be red” will be implemented by the following operations. We find all box nodes whose colors are red in the tree and collect the colors  $g$  of its children nodes, then we change their property vectors  $g$  to  $g'$ , which represents the blue color. Next,  $\mathcal{L}_Y$  is obtained by calculating MSE between all  $g'$  and the original  $g$ . This process is illustrated in C of Figure 2.

In most applications,  $\mathcal{L}_t(x)$  requires much resources to compute, while  $\mathcal{L}_Y$  is efficient to evaluate since it only involves the inference of  $p(x|z; \theta)$ . Thus, we define a proximal operator based on (2),

$$\text{prox}_{\mathcal{L}_Y}(z) = \arg \min_{z'} \left( \mathcal{L}_Y(p(x|z'; \phi), Y_t(x)) + \frac{1}{2} \|z - z'\|_2^2 \right) \quad (12)$$

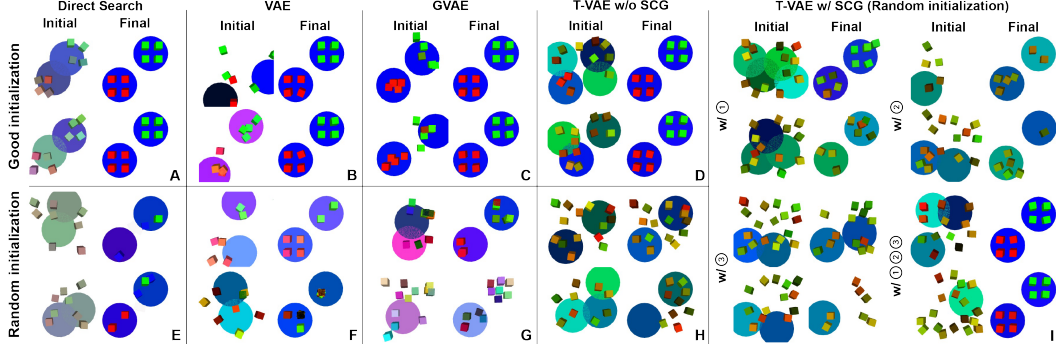


Figure 4: Results of synthetic scene reconstruction experiment from five methods with random and good initialization. **E** shows the results of T-VAE using SCG. With the combination of knowledge ①②③, we can almost reach the optimal solution even from a random initialization, while baseline methods can realize the target *only* when start from the good initialization.

which projects the candidate  $z$  to another point that minimize the knowledge inconsistency caused by  $\mathcal{L}_Y$ . (12) is solved by gradient descent since the decoder  $p(x|z; \theta)$  is differentiable. For the updating step, we can keep using gradient descent (GD) for a differentiable  $L_t(x)$  as shown in (3) or change to black-box optimization methods Audet and Hare [2017] when  $L_t(x)$  is non-differentiable. Finally, the explicit knowledge incorporation and downstream task objective are iteratively optimized under this proximal optimization framework. The complete algorithm is summarized in **Algorithm 1**.

## 4 Experiments

Firstly, we design a synthetic scene to illustrate the controllability and explainability of the proposed framework. The synthetic scene emulates the driving scene with a simplified setting to unveil the essence of the knowledge-guided generation. After that, we propose *Scene Attack* based on SCG and evaluate its performance on semantic adversarial traffic scene generation.

### 4.1 Synthetic Scene Reconstruction

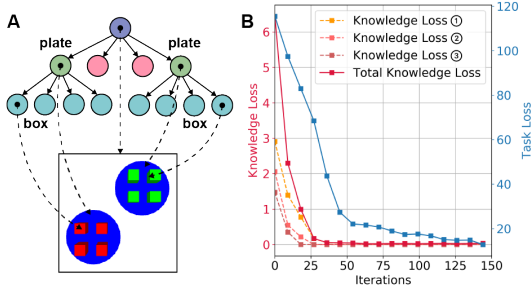


Figure 3: **A** Target scene. **B** Knowledge losses of integrating semantic rules ①②③ separately.

should be smaller than a threshold  $\gamma$ . We compare our method with three baselines: Direct Search (DS), VAE, and Grammar-VAE (GVAE) Kusner et al. [2017]. DS directly optimizes the positions and colors of boxes and plates in the data space. In contrast, VAE and GVAE optimize in the latent space and generate the scene from their decoders. GVAE leverages knowledge by integrating rules during the training stage, however, it cannot explicitly integrate semantic knowledge during the generation.

**Experiment Settings:** DS and VAE need to access the number of boxes and plates in the target image (e.g. 2 plates and 8 boxes) to fix the dimension of the input feature. In contrast, GVAE and T-VAE do not need this assumption. The good initial points for DS are obtained by adding a small

**Task Description:** This task aims to reconstruct a scene from a given image as shown in Figure 3. The task loss minimizes a reconstruction error  $\mathcal{L}_t(x) = \|S - \mathcal{R}(x)\|_2$ , where  $\mathcal{R}$  is a differentiable image renderer Kato et al. [2018] and  $S$  is the image of target scene. Under this clear setting, it is possible to analyze and compares the contribution of explicit knowledge integration, since we can access the optimal solution easily. Based on the target scene, We define three knowledge rules to help with minimizing the task loss: ① The scene has at most two plates; ② The colors of the boxes that belong to the same plate should be the same; ③ The distance between the boxes that belong to the same plate

perturbation to the position and color of the target scene. The good initial points for other methods are obtained by adding a small perturbation to the optimal latent code, which is obtained by passing the target scene to the encoder. We synthesize the training dataset for VAE, GVAE, and T-VAE by randomly generating boxes and plates. The data samples are similar to the target scene but are different in colors and the number of object number, and we repeat the target scene 10 times in the entire 10,000 samples. Since the entire pipeline is differentiable, we use gradient descent to optimize  $\mathcal{L}_t(x)$ .

Table 1: Reconstruction Error

Method	Initialization	
	Random	Good
Direct Search	86.0±9.4	<b>7.9±1.2</b>
VAE	110.4±10.6	13.4±6.1
GVAE	123.7±9.5	19.7±10.2
T-VAE	135.1±16.9	14.1±2.5
T-VAE w/ SCG	<b>14.5±1.3</b>	11.8±2.1

**Evaluation Results:** The generated results from five models are displayed in Figure 4 and Table. 1. With good initial points, all models find a similar scene to the target one, while with random initial points, all models are trapped in local minimums. However, obtaining good initialization is not practical in most real-world applications, indicating that this task is non-trivial and all models without knowledge cannot solve it. After integrating the knowledge into the T-VAE model, we obtain **I** of Figure 4. We can see that all of the

three knowledge have positive guidance for the optimization, e.g., the boxes concentrate on the centers of plates with knowledge ③. When combining the three knowledge, even from a random initialization, our T-VAE with knowledge-enhanced generation can still find the target scene. To explore the contribution of each knowledge during the generation, we plot the knowledge losses of ①②③ in **B** of Figure 3 together with the task loss. We can see that the knowledge losses decrease quickly at the beginning and help optimize the downstream task.

## 4.2 Adversarial Traffic Scenes Generation

**Task Description:** In this task, we aim to generate *realistic* adversarial traffic scenes against point cloud segmentation algorithms, while satisfying certain semantic knowledge rules. To generated adversarial LiDAR scenes containing various fore-/background rather than the point cloud of single 3D object as existing works Lang et al. [2020], Sun et al. [2020a], a couple of challenges should be considered: First, LiDAR scenes with millions of points are hard to be directly operated; Second, generated scenes need to be realistic and follow traffic rules. Since there are no existing baselines to directly compare with, we implement three methods: (1) *Point Attack*: a point-wise attack baseline Xiang et al. [2019] that adds small disturbance to points; (2) *Pose Attack*: a scene generation method developed by us that searches poses of a fixed number of vehicles; (3) *Scene Attack*: a semantically controllable traffic generative method based on our T-VAE and SCG. We explore the attack effectiveness against different models of these methods, as well as their transferability. For *Pose Attack* and *Scene Attack*, we implement an efficient LiDAR model  $\mathcal{R}_p(x, B)$  Möller and Trumbore [1997] (refer to Appendix for details) to convert the generated scene  $x$  to a point cloud scene with an background  $B$ . The task objective  $\min \mathcal{L}_t(x) = \max \mathcal{L}_P(\mathcal{R}(x, B))$  is defined by maximizing the loss function  $\mathcal{L}_P$  of segmentation algorithms  $P$ . We design three explicit knowledge rules: ① roads follow a given layout (location, width, and length); ② vehicles on the lane follow the direction of the lane; ③ vehicles should gather together but keep a certain distance. The reason is that ① ② make sure generated vehicles follow the layout of the background  $B$  and ③ makes the scene contain more vehicles.

**Experiment Settings:** We select 4 point cloud semantic segmentation algorithms (PointNet++ Qi et al. [2017], PolarSeg Zhang et al. [2020], SqueezeSegV3 Xu et al. [2020], Cylinder3D Zhou et al. [2020]) as our victim models, all of which are pre-trained on Semantic Kitti dataset Behley et al. [2019]. We collect two backgrounds  $B$  (Highway and Intersection) in Carla simulator Dosovitskiy et al. [2017]. This background can also be obtained from the real-world sensors to reduce the sim-to-real gap. Since it is usually unable to access the parameters of segmentation algorithms, we focus on the black-box attack in this task. *Point Attack* optimizes  $\mathcal{L}_t(x)$  with SimBA Guo et al. [2019], while *Pose Attack* and *Scene Attack* optimizes  $\mathcal{L}_t(x)$  with Bayesian Optimization (BO) Pelikan et al. [1999]. For the training of T-VAE, We build a dataset by extracting the pose information of vehicles together with road and lane information from Argoverse dataset Chang et al. [2019].



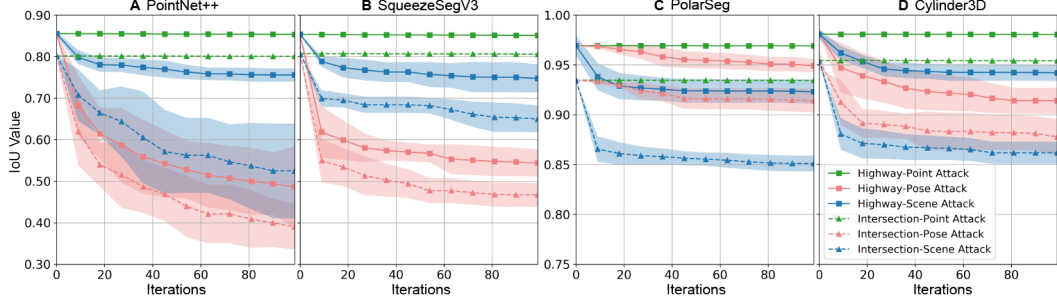


Figure 5: The IoU values during the attack process for four victim models. We compare three methods on two different backgrounds. Highway background is illustrated with solid line and Intersection background is with dash line. Both *Pose Attack* and *Scene Attack* successfully attack all victims.

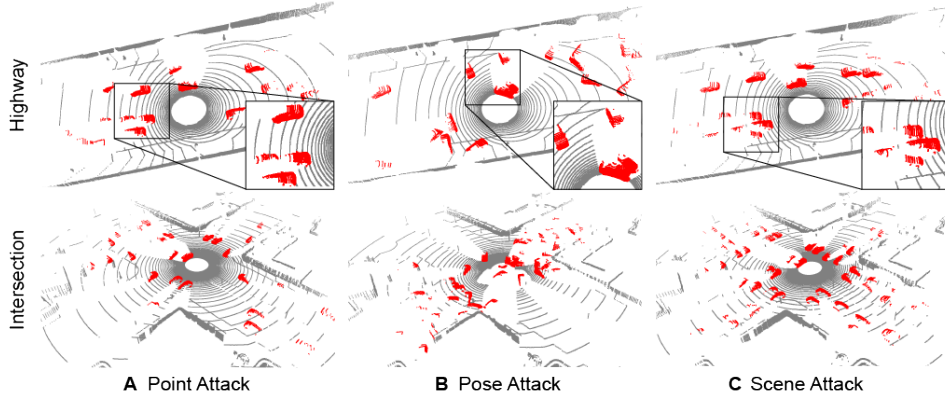


Figure 6: Generated scenes from *Pose Attack* and *Scene Attack* for PointNet++ model under *Highway* and *Intersection* background, where red points represent vehicles. Scenes generated by *Scene Attack* are complicated and follow basic traffic rules, while scenes generated by *Pose Attack* violate basic physical laws and traffic rules.

**Evaluation Results:** We show the Intersection over Union (IoU) metric for the vehicle during the attack in Figure 5. Generally, it is harder to find adversarial scenes in the highway background than in the intersection background since the latter has much more vehicles. Within 100 iterations, *Point Attack* method nearly has no influence to the performance since it operates in very high dimensions. In contrast, *Pose Attack* and *Scene Attack* efficiently reduce the IoU value. Although *Pose Attack* achieves comparable results to our method, scenes generated by it (shown in Figure 6) are unrealistic due to the overlaps between vehicles and traffic rules violation. In contrast, scenes generated by our method (shown in Figure 6) only modify the vehicles within the traffic constraints. In Table 2, we explore the transferability of *Point Attack* and *Scene Attack*. Source models are used to generate scenes, and target models are used to be evaluated. To make the comparison fair, we run 20,000 iterations to get the value for *Point Attack*. Although *Point Attack* method dramatically reduces the performance of all 4 victims, the generated scenes have weak transferability and cannot decrease the performance of other victim models. However, scenes generated by *Scene Attack* successfully attack all models even those not targeted during the training, which demonstrates strong adversarial transferability.

## 5 Related Work

**Incorporating Knowledge in Neural Networks.** Integrating knowledge to data-driven models has been explored in various forms from training methods, meta-modeling, embedding to rules used for reasoning. Hu et al. [2016] distills logical rules with a teacher-student framework under *Posterior Regularization* Ganchev et al. [2010]. Another way of knowledge distillation is encoding knowledge into vectors then refining the features from the model that are in line with the encoded knowledge



Table 2: Transferability of Adversarial Scenes (Point Attack IoU / Scene Attack IoU). *Scene Attack* has lower IoU for all evaluation pairs, which demonstrates its better adversarial transferability.

Source \ Target	PointNet++	SqueezeSegV3	PolarSeg	Cylinder3D
PointNet++	- / -	0.916 / <b>0.768</b>	0.936 / <b>0.854</b>	0.955 / <b>0.918</b>
SqueezeSegV3	0.954 / <b>0.606</b>	- / -	0.932 / <b>0.855</b>	0.956 / <b>0.892</b>
PolarSeg	0.952 / <b>0.528</b>	0.904 / <b>0.753</b>	- / -	0.953 / <b>0.908</b>
Cylinder3D	0.951 / <b>0.507</b>	0.903 / <b>0.688</b>	0.934 / <b>0.877</b>	- / -

Gu et al. [2019]. These methods need to access *Knowledge Graphs* Ehrlinger and Wöß [2016] during the training, which heavily depends on human experts. Meta-modeling of complex fluid is integrated into the neural network to improve the performance of purely data-driven networks in Mahmoudabadbozchelou et al. [2021]. In addition, Yang and Perdikaris [2018] explored restricting generative models’ output to satisfy given physical laws expressed by partial differential equations. In the reinforcement learning area, reward shaping Ng et al. [1999] is recognized as a technique to incorporate heuristic knowledge to guide the training of agents.

**Structured Deep Generative Models.** The original DGMs, such as Generative Adversarial Networks Goodfellow et al. [2014] and Variational Auto-encoder Kingma and Welling [2013], are mostly used for unstructured data. These models make full use of the powerful feature extraction capability of neural networks, thus achieve impressive results Karras et al. [2019], Brock et al. [2018]. However, the physical world is complex and objects in this world have diverse connections. Domain specific structured generative models were developed via tree structures (RvNN-VAE Li et al. [2019]) or graph structure (Graph-VAE Simonovsky and Komodakis [2018]). Rule-based generative models are also explored by sampling from pre-defined rules to form a parse tree Kusner et al. [2017], Kar et al. [2019], Devaranjan et al. [2020]. Typical applications of this kind of model are molecular structure generation Guo and Zhao [2020], Jin et al. [2018, 2020], natural scene generation Para et al. [2020], Deng et al. [2021], and automatic program generation Dai et al. [2018]. Unlike these previous works, our method explicitly integrates knowledge during the generation process. One valuable application of DGMs is generating samples that meet the requirements of downstream tasks Engel et al. [2017], Tripp et al. [2020]. Abdal et al. [2019, 2020] searches in the latent space of StyleGAN Karras et al. [2019] to obtain images that are similar to a given image. For structured data, such a searching framework transforms discrete space optimization into continuous space optimization, which is more efficient Luo et al. [2018]. However, it cannot guarantee the rationality of generated structured data due to the loss of interpretability and constraints in the latent space Dai et al. [2018].

**Scene Generation.** Traditional ways of scene generation focus on sampling from pre-defined rules and grammars, such as probabilistic scene graphs used in Prakash et al. [2019] and heuristic rules applied in Dosovitskiy et al. [2017]. These methods rely on domain expertise and cannot be easily extensible to large-scale scenes. Recently, data-driven generative models Devaranjan et al. [2020], Tan et al. [2021], Para et al. [2020], Li et al. [2019], Kundu et al. [2018] are proposed to learn the distribution of objects and decouple the generation of scene into sequence Tan et al. [2021] and graph Para et al. [2020], Li et al. [2019] of objects. Although they reduce the gap between simulation and reality, generated scenes cannot guarantee to satisfy specific constraints. Another substantial body of literature Eslami et al. [2016], Kosiorek et al. [2018], Gu et al. [2019] explored learning scene graphs from images or generating scene images directly via an end-to-end framework. The understanding and generation of high-dimensional data are extremely difficult, making them less effective than modularized methods Kundu et al. [2018], Wu et al. [2017], Devaranjan et al. [2020].

**Semantically Adversarial Examples.** Early adversarial attack works focused on the pixel-wise attack in the image field, where  $L_p$ -norm is used to constrain the adversarial perturbation. For the sake of the interpretability of the adversarial samples, recent works begin to consider semantic attacks Ding et al. [2021, 2020a, 2018, 2020b]. They attack the rendering process of images by modifying the light condition Liu et al. [2018], Zeng et al. [2019] or manipulating the position and shape of objects Alcorn et al. [2019], Xiao et al. [2019], Jain et al. [2019]. This paper explores the generation of adversarial point cloud scenes, which already has similar prior works Tu et al. [2020], Abdelfattah et al. [2021], Sun et al. [2020b]. Tu et al. [2020], Abdelfattah et al. [2021] modify the environment by adding objects on the top of existing vehicles to make them disappear. Sun et al. [2020b] create a

ghost vehicle by adding an ignoble number of points. However, they simply modify a single object without considering the structural relationship of the whole scene.

## 6 Conclusion

In this paper, we explore semantically controllable data generation tasks with explicit knowledge integration. Inspired by the categorization of knowledge for the scene description, we design a tree-structured generative model to represent structured data. We show that the two types of knowledge can be explicitly injected into the tree structure to guide and restrict the generation process efficiently and effectively. After considering explicit semantic knowledge, we verify that the generated data indeed contain fewer semantic constraint violations. Meanwhile, the generated data still maintain the diversity property and follow its original underlying distribution. Although we focus on the scene generation application, the SCG framework can be extended to other structured data generation tasks, such as chemical molecules and programming languages, which also show hierarchical property. One assumption of this work is that the knowledge is helpful or at least harmless as they are summarized and provided by domain experts, which needs careful examination in the future.

## References

- Rameen Abdal, Yipeng Qin, and Peter Wonka. Image2stylegan: How to embed images into the stylegan latent space? In *Proceedings of the IEEE/CVF International Conference on Computer Vision*, pages 4432–4441, 2019.
- Austin Tripp, Erik Daxberger, and José Miguel Hernández-Lobato. Sample-efficient optimization in the latent space of deep generative models via weighted retraining. *Advances in Neural Information Processing Systems*, 33, 2020.
- Wenhao Ding, Baiming Chen, Bo Li, Kim Ji Eun, and Ding Zhao. Multimodal safety-critical scenarios generation for decision-making algorithms evaluation. *IEEE Robotics and Automation Letters*, 6(2):1551–1558, 2021.
- Ian J Goodfellow, Jean Pouget-Abadie, Mehdi Mirza, Bing Xu, David Warde-Farley, Sherjil Ozair, Aaron Courville, and Yoshua Bengio. Generative adversarial networks. *arXiv preprint arXiv:1406.2661*, 2014.
- Diederik P Kingma and Max Welling. Auto-encoding variational bayes. *arXiv preprint arXiv:1312.6114*, 2013.
- Laurent Dinh, Jascha Sohl-Dickstein, and Samy Bengio. Density estimation using real nvp. *arXiv preprint arXiv:1605.08803*, 2016.
- David Bau, Jun-Yan Zhu, Hendrik Strobelt, Agata Lapedriza, Bolei Zhou, and Antonio Torralba. Understanding the role of individual units in a deep neural network. *Proceedings of the National Academy of Sciences*, 117(48):30071–30078, 2020.
- Antoine Plummerault, Hervé Le Borgne, and Céline Hudelot. Controlling generative models with continuous factors of variations. *arXiv preprint arXiv:2001.10238*, 2020.
- Zoltan Dienes and Josef Perner. A theory of implicit and explicit knowledge. *Behavioral and brain sciences*, 22(5):735–808, 1999.
- David M Blei, Alp Kucukelbir, and Jon D McAuliffe. Variational inference: A review for statisticians. *Journal of the American statistical Association*, 112(518):859–877, 2017.
- Neal Parikh and Stephen Boyd. Proximal algorithms. *Foundations and Trends in optimization*, 1(3): 127–239, 2014.
- Shuhan Tan, Kelvin Wong, Shenlong Wang, Sivabalan Manivasagam, Mengye Ren, and Raquel Urtasun. Scenegan: Learning to generate realistic traffic scenes. *arXiv preprint arXiv:2101.06541*, 2021.

- Manyi Li, Akshay Gadi Patil, Kai Xu, Siddhartha Chaudhuri, Owais Khan, Ariel Shamir, Changhe Tu, Baoquan Chen, Daniel Cohen-Or, and Hao Zhang. Grains: Generative recursive autoencoders for indoor scenes. *ACM Transactions on Graphics (TOG)*, 38(2):1–16, 2019.
- Jayaram Sethuraman. A constructive definition of dirichlet priors. *Statistica sinica*, pages 639–650, 1994.
- Richard Socher, Cliff Chiung-Yu Lin, Andrew Y Ng, and Christopher D Manning. Parsing natural scenes and natural language with recursive neural networks. In *ICML*, 2011.
- Ronald J Williams and David Zipser. A learning algorithm for continually running fully recurrent neural networks. *Neural computation*, 1(2):270–280, 1989.
- Raymond M Smullyan. *First-order logic*. Courier Corporation, 1995.
- Charles Audet and Warren Hare. Derivative-free and blackbox optimization, 2017.
- Hiroharu Kato, Yoshitaka Ushiku, and Tatsuya Harada. Neural 3d mesh renderer. In *Proceedings of the IEEE conference on computer vision and pattern recognition*, pages 3907–3916, 2018.
- Matt J Kusner, Brooks Paige, and José Miguel Hernández-Lobato. Grammar variational autoencoder. In *International Conference on Machine Learning*, pages 1945–1954. PMLR, 2017.
- Itai Lang, Uriel Kotlicki, and Shai Avidan. Geometric adversarial attacks and defenses on 3d point clouds. *arXiv preprint arXiv:2012.05657*, 2020.
- Jiachen Sun, Karl Koenig, Yulong Cao, Qi Alfred Chen, and Z Morley Mao. On the adversarial robustness of 3d point cloud classification. *arXiv preprint arXiv:2011.11922*, 2020a.
- Chong Xiang, Charles R Qi, and Bo Li. Generating 3d adversarial point clouds. In *Proceedings of the IEEE/CVF Conference on Computer Vision and Pattern Recognition*, pages 9136–9144, 2019.
- Tomas Möller and Ben Trumbore. Fast, minimum storage ray-triangle intersection. *Journal of graphics tools*, 2(1):21–28, 1997.
- Charles R Qi, Li Yi, Hao Su, and Leonidas J Guibas. Pointnet++: Deep hierarchical feature learning on point sets in a metric space. *arXiv preprint arXiv:1706.02413*, 2017.
- Yang Zhang, Zixiang Zhou, Philip David, Xiangyu Yue, Zerong Xi, Boqing Gong, and Hassan Foroosh. Polarnet: An improved grid representation for online lidar point clouds semantic segmentation. In *Proceedings of the IEEE/CVF Conference on Computer Vision and Pattern Recognition*, pages 9601–9610, 2020.
- Chenfeng Xu, Bichen Wu, Zining Wang, Wei Zhan, Peter Vajda, Kurt Keutzer, and Masayoshi Tomizuka. Squeezesegv3: Spatially-adaptive convolution for efficient point-cloud segmentation. In *European Conference on Computer Vision*, pages 1–19. Springer, 2020.
- Hui Zhou, Xinge Zhu, Xiao Song, Yuxin Ma, Zhe Wang, Hongsheng Li, and Dahua Lin. Cylinder3d: An effective 3d framework for driving-scene lidar semantic segmentation. *arXiv preprint arXiv:2008.01550*, 2020.
- J. Behley, M. Garbade, A. Milioto, J. Quenzel, S. Behnke, C. Stachniss, and J. Gall. SemanticKITTI: A Dataset for Semantic Scene Understanding of LiDAR Sequences. In *Proc. of the IEEE/CVF International Conf. on Computer Vision (ICCV)*, 2019.
- Alexey Dosovitskiy, German Ros, Felipe Codevilla, Antonio Lopez, and Vladlen Koltun. Carla: An open urban driving simulator. In *Conference on robot learning*, pages 1–16. PMLR, 2017.
- Chuan Guo, Jacob Gardner, Yurong You, Andrew Gordon Wilson, and Kilian Weinberger. Simple black-box adversarial attacks. In *International Conference on Machine Learning*, pages 2484–2493. PMLR, 2019.
- Martin Pelikan, David E Goldberg, Erick Cantú-Paz, et al. Boa: The bayesian optimization algorithm. In *Proceedings of the genetic and evolutionary computation conference GECCO-99*, volume 1, pages 525–532. Citeseer, 1999.

- Ming-Fang Chang, John Lambert, Patsorn Sangkloy, Jagjeet Singh, Slawomir Bak, Andrew Hartnett, De Wang, Peter Carr, Simon Lucey, Deva Ramanan, et al. Argoverse: 3d tracking and forecasting with rich maps. In *Proceedings of the IEEE/CVF Conference on Computer Vision and Pattern Recognition*, pages 8748–8757, 2019.
- Zhiting Hu, Xuezhe Ma, Zhengzhong Liu, Eduard Hovy, and Eric Xing. Harnessing deep neural networks with logic rules. *arXiv preprint arXiv:1603.06318*, 2016.
- Kuzman Ganchev, Joao Graça, Jennifer Gillenwater, and Ben Taskar. Posterior regularization for structured latent variable models. *The Journal of Machine Learning Research*, 11:2001–2049, 2010.
- Jiuxiang Gu, Handong Zhao, Zhe Lin, Sheng Li, Jianfei Cai, and Mingyang Ling. Scene graph generation with external knowledge and image reconstruction. In *Proceedings of the IEEE/CVF Conference on Computer Vision and Pattern Recognition*, pages 1969–1978, 2019.
- Lisa Ehrlinger and Wolfram Wöb. Towards a definition of knowledge graphs. *SEMANTiCS (Posters, Demos, SuCESS)*, 48:1–4, 2016.
- Mohammadamin Mahmoudabadbozchelou, Marco Caggioni, Setareh Shahsavari, William H Hartt, Em Karniadakis, Safa Jamali, et al. Data-driven physics-informed constitutive metamodeling of complex fluids: A multifidelity neural network (mfnn) framework. *Journal of Rheology*, 65(2), 2021.
- Yibo Yang and Paris Perdikaris. Physics-informed deep generative models. *arXiv preprint arXiv:1812.03511*, 2018.
- Andrew Y Ng, Daishi Harada, and Stuart Russell. Policy invariance under reward transformations: Theory and application to reward shaping. In *ICML*, volume 99, pages 278–287, 1999.
- Tero Karras, Samuli Laine, and Timo Aila. A style-based generator architecture for generative adversarial networks. In *Proceedings of the IEEE/CVF Conference on Computer Vision and Pattern Recognition*, pages 4401–4410, 2019.
- Andrew Brock, Jeff Donahue, and Karen Simonyan. Large scale gan training for high fidelity natural image synthesis. *arXiv preprint arXiv:1809.11096*, 2018.
- Martin Simonovsky and Nikos Komodakis. Graphvae: Towards generation of small graphs using variational autoencoders. In *International Conference on Artificial Neural Networks*, pages 412–422. Springer, 2018.
- Amlan Kar, Aayush Prakash, Ming-Yu Liu, Eric Cameracci, Justin Yuan, Matt Rusiniak, David Acuna, Antonio Torralba, and Sanja Fidler. Meta-sim: Learning to generate synthetic datasets. In *Proceedings of the IEEE/CVF International Conference on Computer Vision*, pages 4551–4560, 2019.
- Jeevan Devaranjan, Amlan Kar, and Sanja Fidler. Meta-sim2: Unsupervised learning of scene structure for synthetic data generation. In *European Conference on Computer Vision*, pages 715–733. Springer, 2020.
- Xiaojie Guo and Liang Zhao. A systematic survey on deep generative models for graph generation. *arXiv preprint arXiv:2007.06686*, 2020.
- Wengong Jin, Regina Barzilay, and Tommi Jaakkola. Junction tree variational autoencoder for molecular graph generation. In *International Conference on Machine Learning*, pages 2323–2332. PMLR, 2018.
- Wengong Jin, Regina Barzilay, and Tommi Jaakkola. Hierarchical generation of molecular graphs using structural motifs. In *International Conference on Machine Learning*, pages 4839–4848. PMLR, 2020.
- Wamiq Para, Paul Guerrero, Tom Kelly, Leonidas Guibas, and Peter Wonka. Generative layout modeling using constraint graphs. *arXiv preprint arXiv:2011.13417*, 2020.

- Fei Deng, Zhuo Zhui, Donghun Lee, and Sungjin Ahn. Generative scene graph networks. In *International Conference on Learning Representations*, 2021.
- Hanjun Dai, Yingtao Tian, Bo Dai, Steven Skiena, and Le Song. Syntax-directed variational autoencoder for structured data. *arXiv preprint arXiv:1802.08786*, 2018.
- Jesse Engel, Matthew Hoffman, and Adam Roberts. Latent constraints: Learning to generate conditionally from unconditional generative models. *arXiv preprint arXiv:1711.05772*, 2017.
- Rameen Abdal, Yipeng Qin, and Peter Wonka. Image2stylegan++: How to edit the embedded images? In *Proceedings of the IEEE/CVF Conference on Computer Vision and Pattern Recognition*, pages 8296–8305, 2020.
- Renqian Luo, Fei Tian, Tao Qin, Enhong Chen, and Tie-Yan Liu. Neural architecture optimization. *arXiv preprint arXiv:1808.07233*, 2018.
- Aayush Prakash, Shaad Boochoon, Mark Brophy, David Acuna, Eric Cameracci, Gavriel State, Omer Shapira, and Stan Birchfield. Structured domain randomization: Bridging the reality gap by context-aware synthetic data. In *2019 International Conference on Robotics and Automation (ICRA)*, pages 7249–7255. IEEE, 2019.
- Abhijit Kundu, Yin Li, and James M Rehg. 3d-rcnn: Instance-level 3d object reconstruction via render-and-compare. In *Proceedings of the IEEE conference on computer vision and pattern recognition*, pages 3559–3568, 2018.
- SM Eslami, Nicolas Heess, Theophane Weber, Yuval Tassa, David Szepesvari, Koray Kavukcuoglu, and Geoffrey E Hinton. Attend, infer, repeat: Fast scene understanding with generative models. *arXiv preprint arXiv:1603.08575*, 2016.
- Adam R Kosiorsek, Hyunjik Kim, Ingmar Posner, and Yee Whye Teh. Sequential attend, infer, repeat: Generative modelling of moving objects. *arXiv preprint arXiv:1806.01794*, 2018.
- Jiajun Wu, Joshua B Tenenbaum, and Pushmeet Kohli. Neural scene de-rendering. In *Proceedings of the IEEE Conference on Computer Vision and Pattern Recognition*, pages 699–707, 2017.
- Wenhao Ding, Baiming Chen, Minjun Xu, and Ding Zhao. Learning to collide: An adaptive safety-critical scenarios generating method. In *2020 IEEE/RSJ International Conference on Intelligent Robots and Systems (IROS)*, pages 2243–2250. IEEE, 2020a.
- Wenhao Ding, Wenshuo Wang, and Ding Zhao. A new multi-vehicle trajectory generator to simulate vehicle-to-vehicle encounters. *arXiv preprint arXiv:1809.05680*, 2018.
- Wenhao Ding, Mengdi Xu, and Ding Zhao. Cmts: A conditional multiple trajectory synthesizer for generating safety-critical driving scenarios. In *2020 IEEE International Conference on Robotics and Automation (ICRA)*, pages 4314–4321. IEEE, 2020b.
- Hsueh-Ti Derek Liu, Michael Tao, Chun-Liang Li, Derek Nowrouzezahrai, and Alec Jacobson. Beyond pixel norm-balls: Parametric adversaries using an analytically differentiable renderer. *arXiv preprint arXiv:1808.02651*, 2018.
- Xiaohui Zeng, Chenxi Liu, Yu-Siang Wang, Weichao Qiu, Lingxi Xie, Yu-Wing Tai, Chi-Keung Tang, and Alan L Yuille. Adversarial attacks beyond the image space. In *Proceedings of the IEEE/CVF Conference on Computer Vision and Pattern Recognition*, pages 4302–4311, 2019.
- Michael A Alcorn, Qi Li, Zhitao Gong, Chengfei Wang, Long Mai, Wei-Shinn Ku, and Anh Nguyen. Strike (with) a pose: Neural networks are easily fooled by strange poses of familiar objects. In *Proceedings of the IEEE/CVF Conference on Computer Vision and Pattern Recognition*, pages 4845–4854, 2019.
- Chaowei Xiao, Dawei Yang, Bo Li, Jia Deng, and Mingyan Liu. Meshadv: Adversarial meshes for visual recognition. In *Proceedings of the IEEE/CVF Conference on Computer Vision and Pattern Recognition*, pages 6898–6907, 2019.

- Lakshya Jain, Varun Chandrasekaran, Uyeong Jang, Wilson Wu, Andrew Lee, Andy Yan, Steven Chen, Somesh Jha, and Sanjit A Seshia. Analyzing and improving neural networks by generating semantic counterexamples through differentiable rendering. *arXiv preprint arXiv:1910.00727*, 2019.
- James Tu, Mengye Ren, Sivabalan Manivasagam, Ming Liang, Bin Yang, Richard Du, Frank Cheng, and Raquel Urtasun. Physically realizable adversarial examples for lidar object detection. In *Proceedings of the IEEE/CVF Conference on Computer Vision and Pattern Recognition*, pages 13716–13725, 2020.
- Mazen Abdelfattah, Kaiwen Yuan, Z Jane Wang, and Rabab Ward. Towards universal physical attacks on cascaded camera-lidar 3d object detection models. *arXiv preprint arXiv:2101.10747*, 2021.
- Jiachen Sun, Yulong Cao, Qi Alfred Chen, and Z Morley Mao. Towards robust lidar-based perception in autonomous driving: General black-box adversarial sensor attack and countermeasures. In *29th USENIX Security Symposium (USENIX Security 20)*, pages 877–894, 2020b.